Published in final edited form as:
Mol Cell. 2008 December 05; 32(5): 685–95. doi:10.1016/j.molcel.2008.09.027.

A ncRNA Modulates Histone Modification and mRNA Induction in the Yeast *GAL* Gene Cluster

Jonathan Houseley[1], **Liudmilla Rubbi**[2,3], **Michael Grunstein**[2,*], **David Tollervey**[1,*], **Maria Vogelauer**[1,*]

[1]Wellcome Trust Centre for Cell Biology, Institute for Cell Biology, University of Edinburgh, Edinburgh EH9 3JR, UK

[2]Department of Biological Chemistry, David Geffen School of Medicine at UCLA, Boyer Hall, 611 Charles E. Young Drive, Los Angeles, CA 90095, USA

Summary

The extensively studied yeast *GAL1–10* gene cluster is tightly regulated by environmental sugar availability. Unexpectedly, under repressive conditions the 3′ region of the *GAL10* coding sequence is trimethylated by Set1 on histone H3 K4, normally characteristic of 5′ regions of actively transcribed genes. This reflects transcription of a long noncoding RNA (*GAL10*-ncRNA) that is reciprocal to *GAL1* and *GAL10* mRNAs and driven by the DNA-binding protein Reb1. Point mutations in predicted Reb1-binding sites abolished Reb1 binding and ncRNA synthesis. The *GAL10*-ncRNA is transcribed approximately once every 50 min and targeted for degradation by the TRAMP and exosome complexes, resulting in low steady-state levels (approximately one molecule per 14 cells). *GAL10*-ncRNA transcription recruits the methyltransferase Set2 and histone deacetylation activities *in cis*, leading to stable changes in chromatin structure. These chromatin modifications act principally through the Rpd3S complex to aid glucose repression of *GAL1–10* at physiologically relevant sugar concentrations.

Introduction

Studies of the human and yeast transcriptomes indicate that ncRNAs are much more numerous than initially expected. In metazoans, ncRNAs are implicated in the formation of heterochromatin, X chromosome inactivation, dosage compensation, and allele-specific repression at imprinted loci (reviewed in Munroe and Zhu, 2006; Pauler et al., 2007). However, little is known about the function of the many ncRNA transcripts in euchromatic regions of the genome. The FANTOM3 mouse cDNA sequencing project found many pairs of coding-noncoding transcripts with either coregulation or inverse regulation, suggesting that ncRNAs may play a general role in the regulation of coding transcripts (Katayama et al., 2005). ncRNAs are activated by many of the same factors as coding transcripts; 36% of the predicted binding targets of transcription factors cMyc, Sp1, and p53 occur within or

*Correspondence: mg@mbi.ucla.edu (M.G.), d.tollervey@ed.ac.uk (D.T.), m.vogelauer@ed.ac.uk (M.V.).
[3]Present address: Crump Institute for Molecular Imaging, Department of Molecular and Medical Pharmacology, David Geffen School of Medicine at UCLA, Los Angeles, CA 90095, USA

Europe PMC Funders Author Manuscripts

immediately 3′ to annotated genes, suggesting that they activate antisense transcripts to these coding sequences (Cawley et al., 2004).

Widespread transcription of intergenic regions is also predicted in *S. cerevisiae* from global analyses of RNA pol II density (Steinmetz et al., 2006). ncRNAs derived from intergenic regions and silenced regions of the yeast genome are not normally detected, however, due to the rapid degradation of transcripts by the TRAMP complexes and the nuclear exosome (Houseley et al., 2007; Wyers et al., 2005). Perhaps the best-studied sense-antisense pair is the *PHO84* gene, where loss of the nuclear exosome component Rrp6 leads to stabilization of an anti-sense transcript. This results in repression of the sense transcript through recruitment of the histone deacetylase (HDAC) Hda1, which deacetylates the *PHO84* promoter (Camblong et al., 2007). In addition, ncRNAs repress Ty1 retrotransposition via histone modifications induced *in trans* (Berretta et al., 2008). This suggested that ncRNA transcription could contribute to the establishment of chromatin structure within euchromatic regions.

Histone modifications modulate gene expression by controlling the binding of regulatory proteins (reviewed in Ruthenburg et al., 2007). Nucleosomes are generally hyperacetylated at promoters of active genes and hypoacetylated when transcription is repressed. The process of transcription is accompanied by alterations in histone modification patterns, as chromatin is unfolded in front of, and reassembled behind, the transcribing polymerase. Early transcriptional events lead to localized recruitment of the histone methyltransferase Set1, which trimethylates histone H3 lysine 4 (H3 K4me3) over the 5′ end of transcribed coding regions (Ng et al., 2003; Schneider et al., 2004). As RNA polymerase advances through the gene, lysine 36 of H3 becomes increasingly trimethylated (H3 K36me3) by another histone methyltransferase Set2 (reviewed in Lee and Shilatifard, 2007). This latter modification causes the recruitment of the small Rpd3 HDAC complex, via binding of the chromodomain protein Eaf3, leading to deacetylation over transcribed coding regions and preventing spurious internal transcription initiation (Carrozza et al., 2005; Joshi and Struhl, 2005; Keogh et al., 2005).

The *GAL* cluster of *S. cerevisiae* encodes three genes required for galactose metabolism, *GAL1, GAL7*, and *GAL10*, and has been analyzed extensively as a model for regulated gene expression. The *GAL* cluster has three characterized states depending on the carbon sources available in the medium: induced (in the absence of glucose and the presence of galactose), noninduced (in the absence of glucose and the presence of other carbon sources such as raffinose), and repressed (in the presence of glucose). Such highly regulated nutrient response systems allow *S. cerevisiae* to thrive on a wide range of carbon sources other than fermenting fruit. Analyses of fermented food products have shown *S. cerevisiae* to be commonly the most prevalent microbe in cultures derived from cereals (principle sugar maltose) and milk (principle sugar lactose) (reviewed in Jespersen, 2003). Therefore, *S. cerevisiae* has evolved to metabolize the complex mixtures of sugars present in natural environments.

In this study we demonstrate that binding of the regulatory protein Reb1 to the 3′ end of the *GAL10* ORF stimulates transcription of a ncRNA under repressed and noninduced

conditions. This causes di- and trimethylation of histone 3 lysine 4 (H3 K4me2, H3 K4me3) within the *GAL10* coding region, and H3 K36me3 across the entire *GAL1–10* locus, along with decreased H3 acetylation. These chromatin structure modifications lead to increased glucose repression of *GAL1–10* in low-sugar media, primarily mediated by H3 K36me3 binding protein Eaf3. We suggest that the *GAL10*-ncRNA and other ncRNAs modulate gene expression patterns to optimize nutrient utilization.

Results

H3 K4 Is Methylated over the 3′ Coding Region of *GAL10* under Repressive Conditions

Methylation of histone H3 K4 is closely linked to transcriptional activity of RNA polymerase II (RNA pol II). H3 K4me3 is generally restricted to the 5′ end of transcribed genes, where it correlates with the stable recruitment of the methyltransferase Set1 (Ng et al., 2003). In contrast, H3 K4me2 can spread into the body of genes in higher eukaryotes and appears even more widely distributed in yeast (Pokholok et al., 2005; Santos-Rosa et al., 2002; Schneider et al., 2004). However, we observed an unusual pattern of H3 K4me3 over the *GAL1–10* cluster (Figure 1A).

Chromatin immunoprecipitation (ChIP) was performed across the *GAL1–10* locus on cells grown in inducing medium (2% galactose [GAL]) or repressive medium (2% glucose [GLU]) using antibodies specific to H3 K4me2, H3 K4me3, and HA-tagged Set1. As expected, K4me3 was present over the 5′ end of both *GAL1* and *GAL10* in galactose and correlated with the presence of HA-Set1 (Figures 1B and 1C, left panels). In cells grown on glucose medium, the peaks of K4me2, K4me3, and HA-Set1 binding over the 5′ ends of *GAL1* and *GAL10* disappeared, consistent with repression of the *GAL1–10* promoter (Figures 1B and 1C, right panels). However, a prominent peak of K4me2 and K4me3 appeared over the 3′ coding region of *GAL10*. The same peak was seen in cells grown in noninducing raffinose medium (data not shown). This peak of H3 K4me is not due to increased histone density over the *GAL10-3′* region, as demonstrated by ChIP using an antibody against the C terminus of histone H3 (see Figure S1 available online). Moreover, both K4me2 and K4me3 at this site were abolished in a *set1*Δ strain (Figure S2). However, stable binding of HA-Set1 was not observed over the *GAL10-3′* region, despite the normally tight correlation between Set1 binding to the 5′ end of transcribed genes and the presence of K4me3 (Ng et al., 2003). We conclude that Set1 methylates H3 K4 over the 3′ region of *GAL10* in the absence of induction of the *GAL1–10* promoter.

The Transcription Regulator Reb1 Is Required for H3 K4 Methylation in the 3′ Region of *GAL10*

The presence of H3 K4me2 and H3 K4me3 would not be expected in transcriptionally repressed genes (Ng et al., 2003; Pokholok et al., 2005). We therefore suspected that a DNA binding protein was driving transcription from this region, a hypothesis supported by the presence of a DNase I hypersensitive site in the 3′ region of the *GAL10* ORF (Proffitt, 1985).

Inspection of the DNA sequence identified one perfect consensus binding site for Reb1 (Reb1 BS) and three closely matching sites. Reb1 is a myb-related protein known to be involved in transcription initiation of RNA pol I and II genes and in termination of RNA pol I transcription (Ju et al., 1990; Morrow et al., 1990). ChIP analyses using a genomic Reb1-HA fusion revealed that a peak of Reb1-HA binding was present over the 3′ region of *GAL10* in cells grown in glucose (Figure 2A, GLU) or raffinose medium (data not shown) but was absent in galactose (Figure 2A, GAL). These data correlate well with the presence of the observed H3 K4me peaks, suggesting a causal relation between Reb1 binding and H3 K4 methylation. Extending the analysis to adjacent regions, a second peak of Reb1-HA binding was observed immediately downstream of *GAL7*, corresponding to the position of a further putative Reb1 BS (Figure S3).

Reb1 contains SANT domains, which were previously reported to mediate the binding of c-myb to histone H3 (Mo et al., 2005). It was therefore conceivable that H3 K4me is necessary for the binding of Reb1 to chromatin. However, ChIP analyses demonstrated that Reb1-HA was bound to the 3′ region of *GAL10* in both the wild-type and in *set1*Δ cells that lack H3 K4 methylation (Figure 2B). Conversely, H3 K4 methylation could be a consequence of Reb1 binding to the *GAL10-3′* region. Deletion of *REB1* is lethal, so we abolished its binding to *GAL10* by introducing point mutations into all four putative Reb1-binding sites (Reb1 BSΔ mutant). The resulting strain carrying a mutated *GAL10* grew indistinguishably from the wild-type on standard 2% galactose media. These mutations reduced both the Reb1-HA and K4me2 and -me3 ChIP signals at this locus to background levels (Figures 2C and 2D). We conclude that Reb1 binding in the *GAL10* coding region is required for H3 K4 methylation close to the Reb1-binding site.

Noncoding RNAs in the GAL Cluster

H3 K4me3 is generally associated with sites of transcription initiation, and Reb1 was reported to act as a transcription activator for RNA pol II (Remacle and Holmberg, 1992). To identify Reb1-dependent transcripts, northern blots of RNA from wild-type and Reb1 BSΔ cells grown in glucose and galactose were probed with strand-specific probes to the region of the H3 K4me3 peak (Figure 3A). A major transcript of 4 kb and a weaker 2.3 kb transcript, both running antisense to the *GAL10* gene, were observed in the wild-type strain in glucose but not in galactose medium, consistent with the observed H3 K4 methylation. These transcripts were not detected in the Reb1 BSΔ strain in either sugar. A faint signal from a transcript of 5.6 kb was also observed. This may be related to the additional peak of Reb1-HA binding observed at the 3′ end of *GAL7* (Figure S3). Oligo-dT selection revealed that the ncRNAs are polyadenylated (Figure 3B), and cap-dependent 5′ RACE showed that they are also capped (Figure 3C). Sequencing of cloned 5′ RACE products identified transcription start sites over a 60 bp range between the second and third Reb1-binding sites (Figure 3D).

The major 4 kb ncRNA transcript produced in glucose medium (herein referred to as the *GAL10*-ncRNA) therefore has its promoter at the 3′ end of *GAL10*, runs antisense through the *GAL10* ORF, across the bidirectional *GAL1–10* promoter and extends through *GAL1* in

the sense orientation to its 3′ end (see schematic in Figure 4A). The presence of a 5′ cap and a poly(A) tail strongly suggest that the *GAL10*-ncRNA is produced by RNA pol II.

The half-life of the *GAL10*-ncRNA transcript is ~8 min after addition of 2% galactose to cells growing in 2% raffinose (Figure 3E), suggesting that it is relatively stable. The steadystate level was quantified at ~0.07 molecules per cell, or one transcript in 14 cells, by comparison of hybridization intensity to in vitro transcribed RNA (Figure 3F). The ncRNA was detected at similar levels in cells grown in glucose and raffinose, and in three different wild-type strain backgrounds (data not shown).

Many ncRNAs in *S. cerevisiae* are targeted by the TRAMP4/5 surveillance complexes for rapid degradation immediately after transcription (Wyers et al., 2005). Loss of both poly(A) polymerases of the TRAMP complexes, Trf4 and Trf5, is lethal, so the level of the *GAL* ncRNA was assessed in a conditional *trf4Δ* P_{GAL}*-TRF5* strain 24 hr after transfer to glucose medium. This strain showed a 3.5-fold increase in the abundance of the *GAL10*-ncRNA relative to wildtype (Figure 3G), with a larger increase in the level of the 5.6 kb ncRNA transcript. The abundance of the 5.6 kb transcript was also strongly increased by simultaneous loss of both the Air1 and Air2 components of the TRAMP complexes, which show functionally redundancy (Figure 3G). We conclude that the *GAL10*-ncRNA is targeted for degradation by the TRAMP complexes. Most transcripts are rapidly degraded in the nucleus, but the fraction that escapes nuclear surveillance is relatively stable. Based on the ncRNA half-life and steady-state levels, and compensating for the degraded fraction, we calculate that one transcript is produced per cell every 50 min. Consistent with such a low transcription rate, RNA pol II recruitment to *GAL10* was not detected by ChIP (data not shown).

Expression of the GAL10-ncRNA Modifies Chromatin

Transcription by RNA pol II leads to H3 K36me over coding regions (reviewed in Lee and Shilatifard, 2007). We investigated whether ncRNA transcription is associated with H3 K36me3 over the repressed *GAL1–GAL10* genes. ChIP was performed using antibodies specific to H3 K36me1 or K36me3, and the precipitated DNA was analyzed by PCR with primers scanning the *GAL1–GAL10* region (Figure 4A). In glucose medium, high levels of H3 K36me3 were observed over *GAL10, GAL1*, and the *GAL1–10* promoter region in the strain with the intact Reb1-binding sites (Figure 4B, wild-type). In contrast, only background levels were seen in the Reb1 BSΔ strain (Figure 4B). H3 K36me1 was also elevated over the entire region relative to the internal loading control, but this was independent of the Reb1-binding sites in *GAL10*. We cannot exclude the possibility that the 5.6 kb ncRNA transcript is involved in maintaining this modification. These results show that cryptic ncRNA transcription can direct H3 K36me3 formation over repressed genes and intergenic regions, which otherwise lack this histone modification.

H3 K36me3 is generally associated with subsequent histone deacetylation, so we assessed whether this is the case for *GAL1–GAL10*. Cells were grown in raffinose in order to avoid overlapping histone deacetylation induced by Mig1/Tup1/Hda1-mediated glucose repression. ChIP was performed with antibodies against the acetylated forms of H3 K14/18, H3 K27, and H4 K8, and the chromosomal region encompassing *GAL1* and *GAL10* was

analyzed by PCR in the wild-type and Reb1 BSΔ strains (Figure 4C). The wild-type strain showed reduced H3 K27 acetylation (H3 K27ac) over both the *GAL1* and *GAL10* coding regions relative to the Reb1 BSΔ strain, whereas H3 K14/18ac was clearly decreased only over the *GAL1* coding region, and histone H4 K8ac was marginally altered. We conclude that Reb1-driven ncRNA transcription causes reduced acetylation of specific histone residues over the *GAL1* and *GAL10* coding regions.

GAL10-ncRNA Expression Enhances Glucose Repression

Previously described ncRNAs function in either the activation or repression of transcription (Hongay et al., 2006; Uhler et al., 2007); however, loss of the *GAL10*-ncRNA did not change steady-state levels of *GAL1* or *GAL10* mRNA or their induction rate in standard 2% (20 g l^{-1}) galactose medium (Figures S4A and S4B). Such high galactose concentrations will rarely be encountered by *S. cerevisiae* in the wild, and we therefore suspected that the ncRNA might modulate responses at lower galactose levels. Galactose induction increases between 0.1 g l^{-1} and 1.0 g l^{-1} (Li et al., 2000), and across this range the level of the *GAL10*-ncRNA decreased, suggesting competition with expression of *GAL1–10* (Figure S5A). We selected the lowest concentration that gave clear *GAL1* induction (0.1g l^{-1}) for further analysis, which is physiologically relevant for *S. cerevisiae*, as it falls within the range of galactose concentrations found in grapes (0.05-0.16 g kg^{-1}).

A number of feedback mechanisms operate during galactose induction that may be altered by mutation of the Gal10 protein sequence, despite the Reb1 BSΔ mutant having no discernable growth phenotype on high galactose. To avoid secondary effects from mutation of Gal10, we constructed a second Reb1-binding site mutant (Reb1 BSΔ-silent), which did not change the *GAL10* coding sequence (Figure S6A), and confirmed that this mutant lacked *GAL10*-ncRNA expression by northern blot (Figure 5A) and that H3 K36me3 over *GAL1–10* was reduced (data not shown). As before, this mutant strain showed no difference in *GAL* induction at high galactose concentrations (Figure S6B). This silent Reb1 mutant strain was used for all further experiments.

Induction experiments with wild-type and Reb1 BSΔ-silent using 0.1 g l^{-1} galactose as the sole carbon source revealed only small differences with poor reproducibility (Figure 5A, lanes 1 and 2). We therefore added increasing concentrations of glucose to reveal potential effects of the ncRNA on glucose repression. A clear difference in the level of induction after 3 hr was observed with the addition of 0.1–0.4 g l^{-1} glucose, while addition of 0.8 g l^{-1} glucose repressed induction below detectable levels (Figure 5A). Quantification of induction with 0.1 g l^{-1} galactose for 2 hr in the presence of 0.2 g l^{-1} glucose confirmed a very reproducible difference in mRNA levels (Figure 5B). In three experiments, each with two independent Reb1 BSΔ-silent clones compared to wild-type, mRNA levels were lower in the wild-type than in the mutant ($p < 0.0005$ for *GAL10* mRNA and $p < 0.01$ for *GAL1* mRNA). Across an induction time course (Figures 5C and 5D), this difference was reproducible up to 4–5 hr but became more variable at 5–7 hr, which coincides with the slowed growth at OD > 0.8.

The addition of small quantities of glucose both reduced induction rate and introduced a delay in induction (compare wild-type induction with no glucose [Figure S5B] with

induction in the presence of glucose [Figure 5D]). This explains the difference in wild-type *GAL* induction between 0 g l^{-1} and 0.2 g l^{-1} glucose at 3 hr (Figure 5A, lanes 1 and 5) and 2 hr (Figure 5B, lanes 1 and 3).

The effect of the *GAL10*-ncRNA on histone acetylation and H3 K36me3 over the *GAL1–10* region under these growth conditions is similar to that observed in 2% raffinose, indicating that the same histone modifiers are recruited (Figure S7). Furthermore, H3 K4me3 was increased in the Reb1 BSΔ mutant over *GAL1* in 0.1 g l^{-1} galactose + 0.2 g l^{-1} glucose, presumably reflecting the increased *GAL1* transcription relative to the WT under these growth conditions.

From these data we conclude that the *GAL10*-ncRNA acts to enhance glucose repression of *GAL1–10* induction at low environmental sugar concentrations.

GAL10-ncRNA Enhances Glucose Repression *In Cis* Primarily through Eaf3

Characterized ncRNAs in budding yeast can act both *in cis* (Hongay et al., 2006) and *in trans* (Berretta et al., 2008). If the ncRNA acts *in trans* on *GAL1–10* induction, ncRNA from the wild-type allele in a heterozygous Reb1 BSΔ-silent diploid strain should suppress increased *GAL* induction from the mutant allele, but this will not occur if the ncRNA acts *in cis*. *GAL1–10* induction analysis at the 3 hr time point in these strains revealed that the *GAL10*-ncRNA does not repress induction from a mutant allele *in trans*. A highly significant difference in induction was observed between a homozygous wild-type diploid and a heterozygous Reb1 BSΔ-silent diploid (Figure 6A).

Histone modification analyses were performed in the same heterozygous diploids containing the wild-type and the Reb1 BSΔ-silent allele, along with the parental haploids, using allelespecific PCR primers to the 5′ end of the *GAL10*-ncRNA (Figure S8A). Consistent with *GAL10*-ncRNA being *cis*-acting, H3 K36me3 occurred only over the WT allele (Figure 6B). The two-fold difference in H3 K27 acetylation between wild-type and mutant alleles was maintained in the heterozygous diploid, showing that histone deacetylation also occurs *in cis* (Figures 6B and S8B).

To identify HDACs acting at the *GAL1–10* cluster in WT cells, deletion mutants of nine of the ten known budding yeast HDACs were tested for *GAL1–10* induction with 0.1 g l^{-1} galactose + 0.2 g l^{-1} glucose (Figure 6C). *hos1Δ, hst1Δ, hst2Δ, hst3*Δ, and *hst4*Δ caused detectable but not significant increases in *GAL1–10* induction, as confirmed by the Student's t test. Only *hda1*Δ and *sir2*Δ significantly affected *GAL1–10* expression under these conditions and were chosen for further investigation (Figure 6C). The remaining HDAC, Rpd3, could not be tested in this assay as it conferred a mild slow growth phenotype that interfered with the interpretation of induction data. Nevertheless, ChIP analyses in raffinose showed that deletion of *RPD3* led to increased H3 K27 acetylation. Neither H3 K9 nor H3 K14/K18 acetylation were affected, likely due to redundancy with other HDACs (Figure S9). These data suggested that the *GAL10*-ncRNA acts through recruitment of Hda1, Sir2, or Rpd3.

If one HDAC were directly recruited by the *GAL10*-ncRNA, its absence should cause increased *GAL1–10* induction—but this should not be additive with the Reb1 BSΔ mutation. To test this possibility, *HDA1* and *SIR2* were deleted in WT and Reb1 BSΔ-silent strain backgrounds, and *GAL1–10* induction was tested as described above. Since *rpd3*Δ could not be analyzed by *GAL* induction, we instead deleted *EAF3*, a subunit of the Rpd3S complex, which did not cause any detectable growth phenotype.

The *hda1*Δ deletion increased *GAL1–10* induction in WT cells but had a much greater effect in the Reb1 BSΔ-silent strain (Figure 6D), showing that Hda1 acts synergistically with the *GAL10*-ncRNA. ChIP analysis of wild-type and *hda1*Δ cells growing in 2% raffinose also revealed a synergistic effect between Hda1 and the *GAL10*-ncRNA on H3 K14/18 acetylation (Figure S9). Since the effects of the *GAL10*-ncRNA are seen in the absence of Hda1, this cannot be a major downstream target of the ncRNA. Hda1 was previously shown to aid glucose repression through its interaction with the Tup1/Ssn6 corepressor (Wu et al., 2001). Recruitment of this complex to *GAL1–10* by the glucose repressors Mig1 and Nrg1 may explain the observed increase in H3 K14/18ac and *GAL1–10* derepression in *hda1*Δ cells.

The *sir2*Δ deletion increased *GAL1–10* induction in the WT and the Reb1 BSΔ-silent strains to similar levels. However, loss of Sir2 also reproducibly reduced expression of the *GAL10*-ncRNA (Figures 6C and 6D). This suggests that depression of *GAL1–10* in *sir2*Δ partly reflects the loss of the ncRNA. Derepression of *GAL1–10* in the *sir2*Δ strain was, however, stronger than that in the Reb1-BSΔ-silent mutants, indicating that the effects of *sir2*Δ are not solely due to loss of *GAL10*-ncRNA synthesis. The basis of the requirement for Sir2 in production of the *GAL10*-ncRNA is currently unclear but does not simply reflect interference from the increased *GAL1–10* transcription (Figures 6C and 6D compare *GAL10*-ncRNA levels in *sir2*Δ and *hda1*Δ, which show similar *GAL10* mRNA). Sir2 activity is NAD+ dependent, and these data may be related to recently reported effects of the cellular NAD/NADP ratio on *GAL1–10* expression (Kumar et al., 2008).

The *eaf3*Δ mutation greatly reduced the difference between the wild-type and the Reb1 BSΔ strain (on average across seven experiments) (Figure 6D), indicating that Eaf3 is required for the effects of the *GAL10*-ncRNA on *GAL1–10* expression. Over other transcribed regions, Eaf3 binds to H3 K36me3 and recruits the Rpd3S HDAC complex, and subsequent deacetylation then acts to inhibit spurious transcription initiation. We conclude that the *GAL10*-ncRNA acts *in cis* through a similar mechanism, with transcription-coupled deposition of H3 K36me3 leading to histone deacetylation by Rpd3S and increased glucose repression of *GAL1–10* under low-glucose conditions.

Discussion

Reb1 Drives ncRNA Transcription

Recent studies have suggested that noncoding transcripts are so common in budding yeast that almost the entire genome is transcribed by RNA pol II (Steinmetz et al., 2006), making it an excellent system for their functional analysis. We here show that binding of the transcription factor Reb1 within the *GAL10* coding region drives the expression of an

antisense transcript covering almost the entire *GAL1–10* locus under noninduced or repressing conditions (Figure 7).

Reb1 is an essential protein initially identified as a Pol I transcription termination and initiation factor (Morrow et al., 1990) and subsequently shown to stimulate RNA pol II transcription at many housekeeping genes (Graham and Chambers, 1994; Packham et al., 1996; Remacle and Holmberg, 1992; Schuller et al., 1994; Yagi et al., 1994). The role of Reb1 in driving ncRNA transcription is unlikely to be restricted to the *GAL* locus. The consensus Reb1-binding site (CGGGTAA) can be identified close to the initiation site of the *PHO84* antisense transcript, and further inter-genic Reb1 binding targets were detected in a whole-genome study using ChIP-on-chip (Harbison et al., 2004). BLAST searches reveal 215 perfect matches to the Reb1-binding sequence within coding regions in *S. cerevisiae* (see Figure S5). In addition, Reb1 acts in the rDNA and as an insulator at subtelomeric Y′ elements (Fourel et al., 2001; Fourel et al., 1999; Kulkens et al., 1992). Recent studies have identified ncRNAs in both the rDNA and telomeric regions with transcriptional start sites in close proximity to Reb1-binding sites (Houseley et al., 2007; Li et al., 2006; Vasiljeva et al., 2008). We speculate that Reb1 may also act in these regions through the induction of ncRNAs and concomitant long-range changes in chromatin structure.

Transcription of the ncRNA Alters the Chromatin Structure *In Cis*

ncRNAs can act *in cis*, in which case their function is limited to the genomic region of their production, or *in trans*, targeting chromosomal loci with sequence similarity to the ncRNA itself. A role for the *GAL10*-ncRNA as a diffusible, *trans*-acting factor seemed unlikely, due to its low steady-state level of ~0.07 copies per cell. This was confirmed by analyses in a heterozygous diploid, which showed that only the chromosome expressing the ncRNA was subject to its effects.

Transcription of the *GAL10*-ncRNA was estimated to occur only once every 50 min on average. Despite its apparently infrequent expression, *GAL10*-ncRNA transcription profoundly altered the chromatin structure over the *GAL1* and *GAL10* genes (Figure 7). By specifically mutating the Reb1-binding sites, we were able to investigate histone modifications directly caused by the transcript. As with other RNA pol II transcribed regions, nucleosomes over the 5′ end of the *GAL10*-ncRNA were di- and trimethylated at H3 K4 by the methyltransferase Set1. Stable binding of Set1 was not detected by ChIP, probably as a result of the low frequency of ncRNA transcription.

Most previously characterized repressive ncRNAs in yeast such as *SRG1*, which regulates *SER3*, act via a transcriptional interference mechanism, whereby high-level transcription through the promoter region of a coding gene interferes with transcription factor binding (Martens et al., 2004). The low transcription frequency of the *GAL10* ncRNA indicates that this mechanism is unlikely to make a substantial contribution to the observed *GAL* regulation, and a mechanism involving persistent histone modification was therefore sought.

Over transcribed protein-coding regions, RNA pol II elongation induces H3 K36me3, which is important for repression of spurious transcription initiation within transcribed regions (Carrozza et al., 2005; Joshi and Struhl, 2005; Keogh et al., 2005). We detected H3 K36me3

over the entire region covered by the ncRNA transcript in the wild-type, but not in the Reb1-BSΔ mutant strain. H3 K36me3 has been shown to recruit the Rpd3S HDAC complex, leading to histone deacetylation (Carrozza et al., 2005; Joshi and Struhl, 2005; Keogh et al., 2005). Indeed, histone acetylation was increased at all analyzed lysine residues in the Reb1-BSΔ mutant strain. Analysis of acetylation levels further confirmed a role of Rpd3 in deacetylating lysine residues over the *GAL1–10* region (Figure S9). Therefore, the rarely transcribed *GAL10*-ncRNA induces histone modification patterns otherwise associated only with strongly transcribed coding regions.

The differences in histone acetylation induced by the ncRNA were more marked over the *GAL1* and *GAL10* ORFs than over the actual *GAL1–10* promoter. This suggests that the alterations in *GAL* induction either result from changes in promoter clearance or transcription elongation, or are due to effects at a distance, such as perturbation of the formation of gene loops or other active chromatin conformations.

Over protein-coding genes, the Rpd3S HDAC complex is recruited by the H3 K36me3-binding protein Eaf3 (Carrozza et al., 2005; Joshi and Struhl, 2005; Keogh et al., 2005). Deletion of *EAF3* caused derepression *GAL1–10* in low-glucose conditions, which was not further increased by the Reb1 BSΔ-silent mutation. This indicates that the effects of the *GAL10*-ncRNA on *GAL1–10* expression require the activity of Eaf3, consistent with recruitment of Rpd3S. The yeast genome encodes nine other putative HDACs, and all of these were also tested for effects on *GAL1–10* induction. Of these, loss of Hda1 showed synergistic enhancement of *GAL1–10* expression under the low-glucose conditions, indicating that it functions in parallel with the ncRNA/Rpd3S pathway. Loss of Sir2 resulted in the reduction of the *GAL10*-ncRNA, via a currently unknown mechanism, and this was accompanied by derepression of *GAL1–10*. No other HDAC mutation suppressed the effects of the loss of the *GAL10*-ncRNA, consistent with the model that this acts predominately through Eaf3/Rpd3S.

These data support the model shown in Figure 7. Reb1-driven transcription of the *GAL10*-ncRNA leads to K36 trimethylation of histone H3. This recruits the Rpd3S complex via the H3 K36me3-binding protein Eaf3, leading to increased deacetylation across the *GAL1–10* locus and increased repression of the divergent *GAL1–10* promoter. Moreover, this mechanism is probably not restricted to *GAL1–10*. Preliminary analysis of the remaining core gene of the *GAL* operon, *GAL2*, revealed a peak of H3 K4me3 at the 3′ end of the ORF and a corresponding ncRNA that runs antisense to the entire *GAL2* gene (data not shown).

The phenotypic consequences of *GAL10*-ncRNA expression were not manifested during growth in standard laboratory media. However, clear differences in *GAL1–10* expression were detected in glucose-galactose mixtures, which may represent more physiological conditions. In fact, most natural substrates will contain complex mixtures of nutrients, many present at low levels. This suggested that antisense ncRNAs might participate in the regulation of many metabolic genes and would be detectable as peaks of H3 K4me3 at the 3′ end of the open reading frames. Examination of published ChIP-on-chip data (Kirmizis et al., 2007) revealed peaks of H3 K4me3 at the 3′ end of ORFs of many glucose-repressed

metabolic genes, including *HXT[8, 13, 15, 16*, and *17*], *MPH2, MPH3, JEN1*, *ICL2*, and *ICL1*. This strongly suggests that ncRNAs participate in the regulation of multiple catabolic genes, acting collectively to optimize gene expression in response to the complex and rapidly changing mix of nutrients available to yeast populations growing on natural substrates.

Experimental Procedures

Strains and Media

Strains were constructed by standard methods and are listed in Table S1; details are given in the Supplemental Data. For ChIP analysis, colonies from YPD (2% glucose) plates were pregrown overnight in YPD (2% glucose), YPR (2% raffinose), or YPG (2% galactose), diluted into the same media to OD_{600} 0.25 and grown to OD_{600} 1. For RNA analysis, cells were grown at 30° to OD_{600} 0.2–0.6 in rich media (1% yeast extract, 2% peptone, 2% sugar), except for in Figure S4B, where synthetic media was used (0.5% NH_4SO_4, 0.17% yeast nitrogen base, 1 × amino acids, 2% sugar). For highly reproducible longer (3 hr) *GAL* inductions, cells were grown overnight to OD 0.2–0.5 in YPR and diluted to precisely OD 0.2 prior to induction at 15 s intervals with glucose/galactose mixtures.

ChIP

ChIP and PCR conditions were essentially as described in Suka et al. (2001). Primer sequences are indicated in Table S3. Additional washings (3×10 min) with lysis buffer previous to sonication were used with αHA antibody and initial 140 mM NaCl concentration was adjusted to 275 mM for incubation with αHA antibody. Antibodies used are described in Table S4.

RNA Methods

Cells were fixed by addition of ethanol to 70% prior to RNA extraction, and northern blotting and probing were performed as described (Houseley et al., 2007). Details of hybridization conditions are given in the Supplemental Data.

Supplementary Material

Refer to Web version on PubMed Central for supplementary material.

Acknowledgments

We thank Kevin Struhl for providing the FT4 WT and HA-Set1 strains. J.H. was funded by the Leverhulme Trust, D.T. was funded by The Wellcome Trust, L.R. and M.G. were funded by NIH GM23674, and M.V. was funded by NIH GM23674 and The Wellcome Trust MV37766. We thank the members of the Grunstein, Tollervey, and Vogelauer labs for helpful discussions.

References

Berretta J, Pinskaya M, Morillon A. A cryptic unstable transcript mediates transcriptional trans-silencing of the Ty1 retrotransposon in S. cerevisiae. Genes Dev. 2008; 22:615–626. [PubMed: 18316478]

Camblong J, Iglesias N, Fickentscher C, Dieppois G, Stutz F. Antisense RNA stabilization induces transcriptional gene silencing via histone deacetylation in S. cerevisiae. Cell. 2007; 131:706–717. [PubMed: 18022365]

Carrozza MJ, Li B, Florens L, Suganuma T, Swanson SK, Lee KK, Shia WJ, Anderson S, Yates J, Washburn MP, Workman JL. Histone H3 methylation by Set2 directs deacetylation of coding regions by Rpd3S to suppress spurious intragenic transcription. Cell. 2005; 123:581–592. [PubMed: 16286007]

Cawley S, Bekiranov S, Ng HH, Kapranov P, Sekinger EA, Kampa D, Piccolboni A, Sementchenko V, Cheng J, Williams AJ, et al. Unbiased mapping of transcription factor binding sites along human chromosomes 21 and 22 points to widespread regulation of noncoding RNAs. Cell. 2004; 116:499–509. [PubMed: 14980218]

Fourel G, Revardel E, Koering CE, Gilson E. Cohabitation of insulators and silencing elements in yeast subtelomeric regions. EMBO J. 1999; 18:2522–2537. [PubMed: 10228166]

Fourel G, Boscheron C, Revardel E, Lebrun E, Hu YF, Simmen KC, Muller K, Li R, Mermod N, Gilson E. An activation-independent role of transcription factors in insulator function. EMBO Rep. 2001; 2:124–132. [PubMed: 11258704]

Graham IR, Chambers A. A Reb1p-binding site is required for efficient activation of the yeast RAP1 gene, but multiple binding sites for Rap1p are not essential. Mol Microbiol. 1994; 12:931–940. [PubMed: 7934900]

Harbison CT, Gordon DB, Lee TI, Rinaldi NJ, Macisaac KD, Danford TW, Hannett NM, Tagne JB, Reynolds DB, Yoo J, et al. Transcriptional regulatory code of a eukaryotic genome. Nature. 2004; 431:99–104. [PubMed: 15343339]

Hongay CF, Grisafi PL, Galitski T, Fink GR. Antisense transcription controls cell fate in Saccharomyces cerevisiae. Cell. 2006; 127:735–745. [PubMed: 17110333]

Houseley J, Kotovic K, El Hage A, Tollervey D. Trf4 targets ncRNAs from telomeric and rDNA spacer regions and functions in rDNA copy number control. EMBO J. 2007; 26:4996–5006. [PubMed: 18007593]

Jespersen L. Occurrence and taxonomic characteristics of strains of Saccharomyces cerevisiae predominant in African indigenous fermented foods and beverages. FEM Yeast Res. 2003; 3:191–200.

Joshi AA, Struhl K. Eaf3 chromodomain interaction with methylated H3-K36 links histone deacetylation to Pol II elongation. Mol Cell. 2005; 20:971–978. [PubMed: 16364921]

Ju QD, Morrow BE, Warner JR. REB1, a yeast DNA-binding protein with many targets, is essential for growth and bears some resemblance to the oncogene myb. Mol Cell Biol. 1990; 10:5226–5234. [PubMed: 2204808]

Katayama S, Tomaru Y, Kasukawa T, Waki K, Nakanishi M, Nakamura M, Nishida H, Yap CC, Suzuki M, Kawai J, et al. Antisense transcription in the mammalian transcriptome. Science. 2005; 309:1564–1566. [PubMed: 16141073]

Keogh MC, Kurdistani SK, Morris SA, Ahn SH, Podolny V, Collins SR, Schuldiner M, Chin K, Punna T, Thompson NJ, et al. Cotranscriptional set2 methylation of histone H3 lysine 36 recruits a repressive Rpd3 complex. Cell. 2005; 123:593–605. [PubMed: 16286008]

Kirmizis A, Santos-Rosa H, Penkett CJ, Singer MA, Vermeulen M, Mann M, Bahler J, Green RD, Kouzarides T. Arginine methylation at histone H3R2 controls deposition of H3K4 trimethylation. Nature. 2007; 449:928–932. [PubMed: 17898715]

Kulkens T, van der Sande CA, Dekker AF, van Heerikhuizen H, Planta RJ. A system to study transcription by yeast RNA polymerase I within the chromosomal context: functional analysis of the ribosomal DNA enhancer and the RBP1/REB1 binding sites. EMBO J. 1992; 11:4665–4674. [PubMed: 1425596]

Kumar PR, Yu Y, Sternglanz R, Johnston SA, Joshua-Tor L. NADP regulates the yeast GAL induction system. Science (New York, NY. 2008; 319:1090–1092.

Lee JS, Shilatifard A. A site to remember: H3K36 methylation a mark for histone deacetylation. Mutat Res. 2007; 618:130–134. [PubMed: 17346757]

Li J, Wang S, VanDusen WJ, Schultz LD, George HA, Herber WK, Chae HJ, Bentley WE, Rao G. Green fluorescent protein in Saccharomyces cerevisiae: real-time studies of the GAL1 promoter. Biotechnol Bioeng. 2000; 70:187–196. [PubMed: 10972930]

Li C, Mueller JE, Bryk M. Sir2 represses endogenous polymerase II transcription units in the ribosomal DNA nontranscribed spacer. Mol Biol Cell. 2006; 17:3848–3859. [PubMed: 16807355]

Martens JA, Laprade L, Winston F. Intergenic transcription is required to repress the Saccharomyces cerevisiae SER3 gene. Nature. 2004; 429:571–574. [PubMed: 15175754]

Mo X, Kowenz-Leutz E, Laumonnier Y, Xu H, Leutz A. Histone H3 tail positioning and acetylation by the c-Myb but not the v-Myb DNA-binding SANT domain. Genes Dev. 2005; 19:2447–2457. [PubMed: 16195416]

Morrow BE, Ju Q, Warner JR. Purification and characterization of the yeast rDNA binding protein REB1. J Biol Chem. 1990; 265:20778–20783. [PubMed: 2249986]

Munroe SH, Zhu J. Overlapping transcripts, double-stranded RNA and antisense regulation: a genomic perspective. Cell Mol Life Sci. 2006; 63:2102–2118. [PubMed: 16847578]

Ng HH, Robert F, Young RA, Struhl K. Targeted recruitment of Set1 histone methylase by elongating Pol II provides a localized mark and memory of recent transcriptional activity. Mol Cell. 2003; 11:709–719. [PubMed: 12667453]

Packham EA, Graham IR, Chambers A. The multifunctional transcription factors Abf1p, Rap1p and Reb1p are required for full transcriptional activation of the chromosomal PGK gene in Saccharomyces cerevisiae. Mol Gen Genet. 1996; 250:348–356. [PubMed: 8602150]

Pauler FM, Koerner MV, Barlow DP. Silencing by imprinted noncoding RNAs: is transcription the answer? Trends Genet. 2007; 23:284–292. [PubMed: 17445943]

Pokholok DK, Harbison CT, Levine S, Cole M, Hannett NM, Lee TI, Bell GW, Walker K, Rolfe PA, Herbolsheimer E, et al. Genomewide map of nucleosome acetylation and methylation in yeast. Cell. 2005; 122:517–527. [PubMed: 16122420]

Proffitt JH. DNase I-hypersensitive sites in the galactose gene cluster of Saccharomyces cerevisiae. Mol Cell Biol. 1985; 5:1522–1524. [PubMed: 3897838]

Remacle JE, Holmberg S. A REB1-binding site is required for GCN4-independent ILV1 basal level transcription and can be functionally replaced by an ABF1-binding site. Mol Cell Biol. 1992; 12:5516–5526. [PubMed: 1448083]

Ruthenburg AJ, Li H, Patel DJ, Allis CD. Multivalent engagement of chromatin modifications by linked binding modules. Nat Rev Mol Cell Biol. 2007; 8:983–994. [PubMed: 18037899]

Santos-Rosa H, Schneider R, Bannister AJ, Sherriff J, Bernstein BE, Emre NC, Schreiber SL, Mellor J, Kouzarides T. Active genes are tri-methylated at K4 of histone H3. Nature. 2002; 419:407–411. [PubMed: 12353038]

Schneider R, Bannister AJ, Myers FA, Thorne AW, Crane-Robinson C, Kouzarides T. Histone H3 lysine 4 methylation patterns in higher eukaryotic genes. Nat Cell Biol. 2004; 6:73–77. [PubMed: 14661024]

Schuller HJ, Schutz A, Knab S, Hoffmann B, Schweizer E. Importance of general regulatory factors Rap1p, Abf1p and Reb1p for the activation of yeast fatty acid synthase genes FAS1 and FAS2. Eur J Biochem. 1994; 225:213–222. [PubMed: 7925441]

Steinmetz EJ, Warren CL, Kuehner JN, Panbehi B, Ansari AZ, Brow DA. Genome-wide distribution of yeast RNA polymerase II and its control by Sen1 helicase. Mol Cell. 2006; 24:735–746. [PubMed: 17157256]

Suka N, Suka Y, Carmen AA, Wu J, Grunstein M. Highly specifc antibodies determine histone acetylation site usage in yeast heterochromatin and euchromatin. Mol Cell. 2001; 8:473–479. [PubMed: 11545749]

Uhler JP, Hertel C, Svejstrup JQ. A role for noncoding transcription in activation of the yeast PHO5 gene. Proc Natl Acad Sci USA. 2007; 104:8011–8016. [PubMed: 17470801]

Vasiljeva L, Kim M, Terzi N, Soares LM, Buratowski S. Transcription termination and RNA degradation contribute to silencing of RNA polymerase II transcription within heterochromatin. Mol Cell. 2008; 29:313–323. [PubMed: 18280237]

Wu J, Suka N, Carlson M, Grunstein M. TUP1 utilizes histone H3/H2B-specifc HDA1 deacetylase to repress gene activity in yeast. Mol Cell. 2001; 7:117–126. [PubMed: 11172717]

Wyers F, Rougemaille M, Badis G, Rousselle JC, Dufour ME, Boulay J, Regnault B, Devaux F, Namane A, Seraphin B, et al. Cryptic pol II transcripts are degraded by a nuclear quality control pathway involving a new poly(A) polymerase. Cell. 2005; 121:725–737. [PubMed: 15935759]

Yagi S, Yagi K, Fukuoka J, Suzuki M. The UAS of the yeast GAPDH promoter consists of multiple general functional elements including RAP1 and GRF2 binding sites. J Vet Med Sci. 1994; 56:235–244. [PubMed: 8075210]

Europe PMC Funders Author Manuscripts

Europe PMC Funders Author Manuscripts

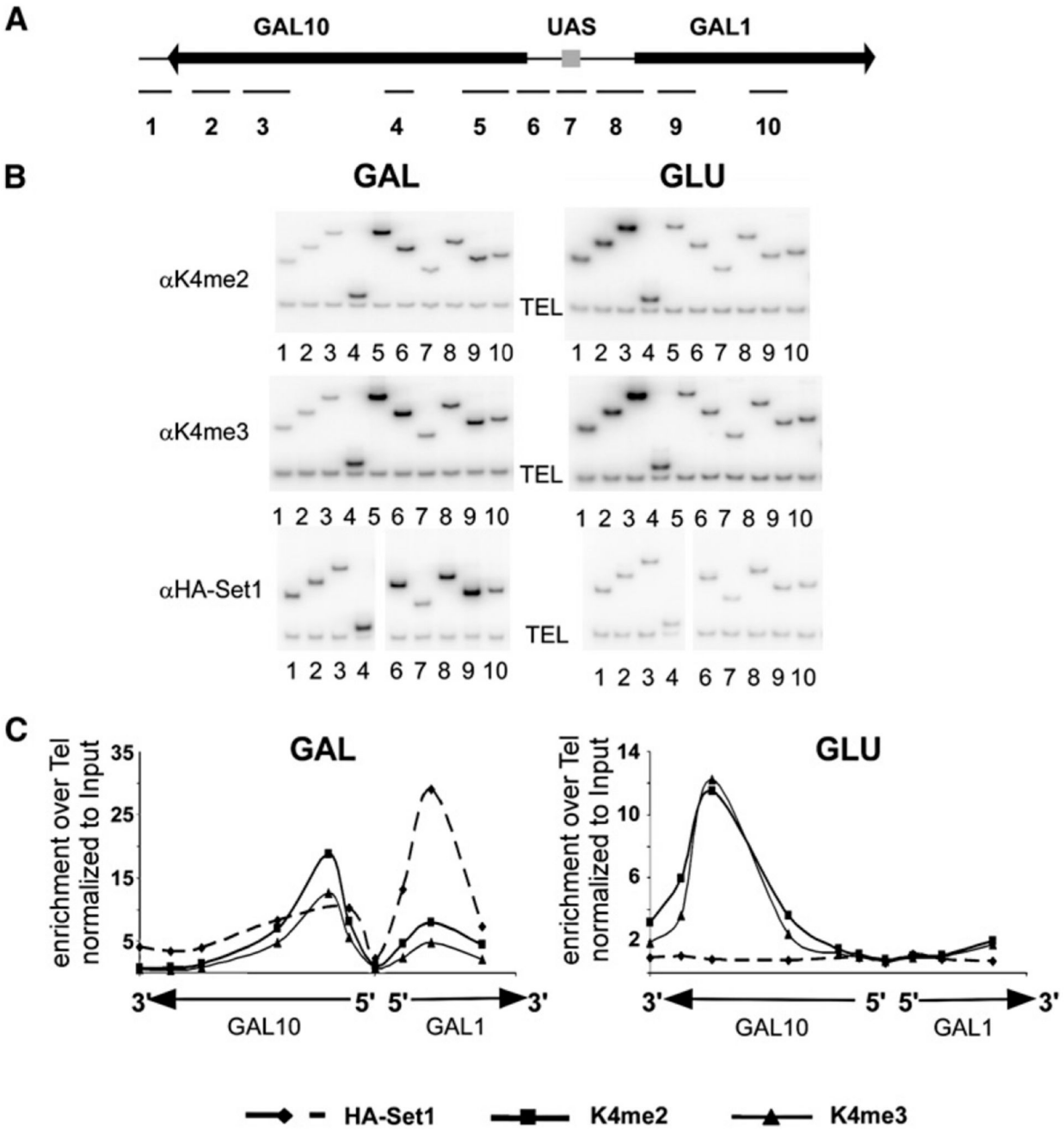

Figure 1. H3 K4 Methylation Pattern at the *GAL1–GAL10* Locus

(A) Schematic of the *GAL* locus showing the location of primer sets used for ChIP analysis. (B) ChIP analysis of H3 K4 methylation and HA-Set1 binding. Cells were grown to log phase in rich media containing 2% galactose (GAL) or 2% glucose (GLU), and chromatin was precipitated with antibodies to H3 K4me2, H3 K4me3, and the HA-epitope. PCR was performed with primer sets shown in (A) and a telomeric primer set (TEL) as a loading control.

(C) Quantification of ChIP data as fold enrichment of signal at the *GAL* locus over telomeric signal normalized to the input.

Europe PMC Funders Author Manuscripts

Europe PMC Funders Author Manuscripts

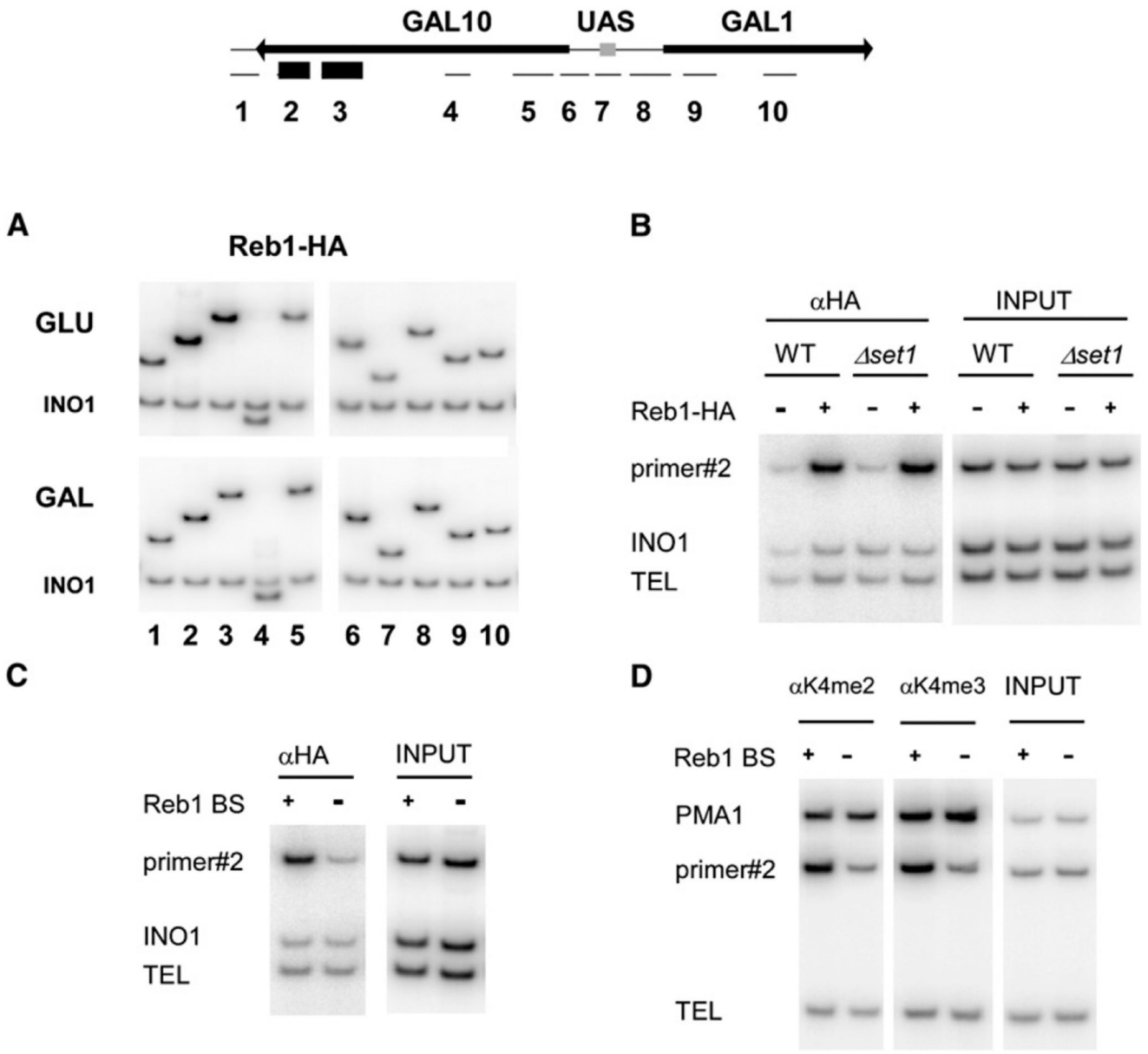

Figure 2. Reb1 Binding to *GAL10* in Glucose Causes H3 K4 Methylation

(A) ChIP analysis of Reb1-HA binding at the *GAL* locus in 2% glucose (GLU) and 2% galactose (GAL) medium, performed as in Figure 1. Primers are shown in schematic (top). A PCR primer set to the *INO1* coding region was used as internal loading control.

(B) ChIP analysis of Reb1-HA binding at the *GAL* locus in wild-type and *set1*Δ cells grown in glucose media, performed as in Figure 1.

(C) Reb1-HA binding in the presence and absence of Reb1-binding sites (Reb1 BS+/−) is shown by ChIP from cells grown in glucose media. Primer #2 was used to amplify the *GAL* locus. Primer sets to the *INO1* coding region (INO1) and a telomeric DNA (TEL) were used as loading controls.

(D) ChIP analysis of H3 K4 methylation at the *GAL* locus in wild-type and Reb1 BSΔ mutant grown in glucose media. ChIP analysis was performed as in Figure 1; primer sets to *PMA1* and TEL act as positive and negative controls for H3 K4 methylation.

Europe PMC Funders Author Manuscripts

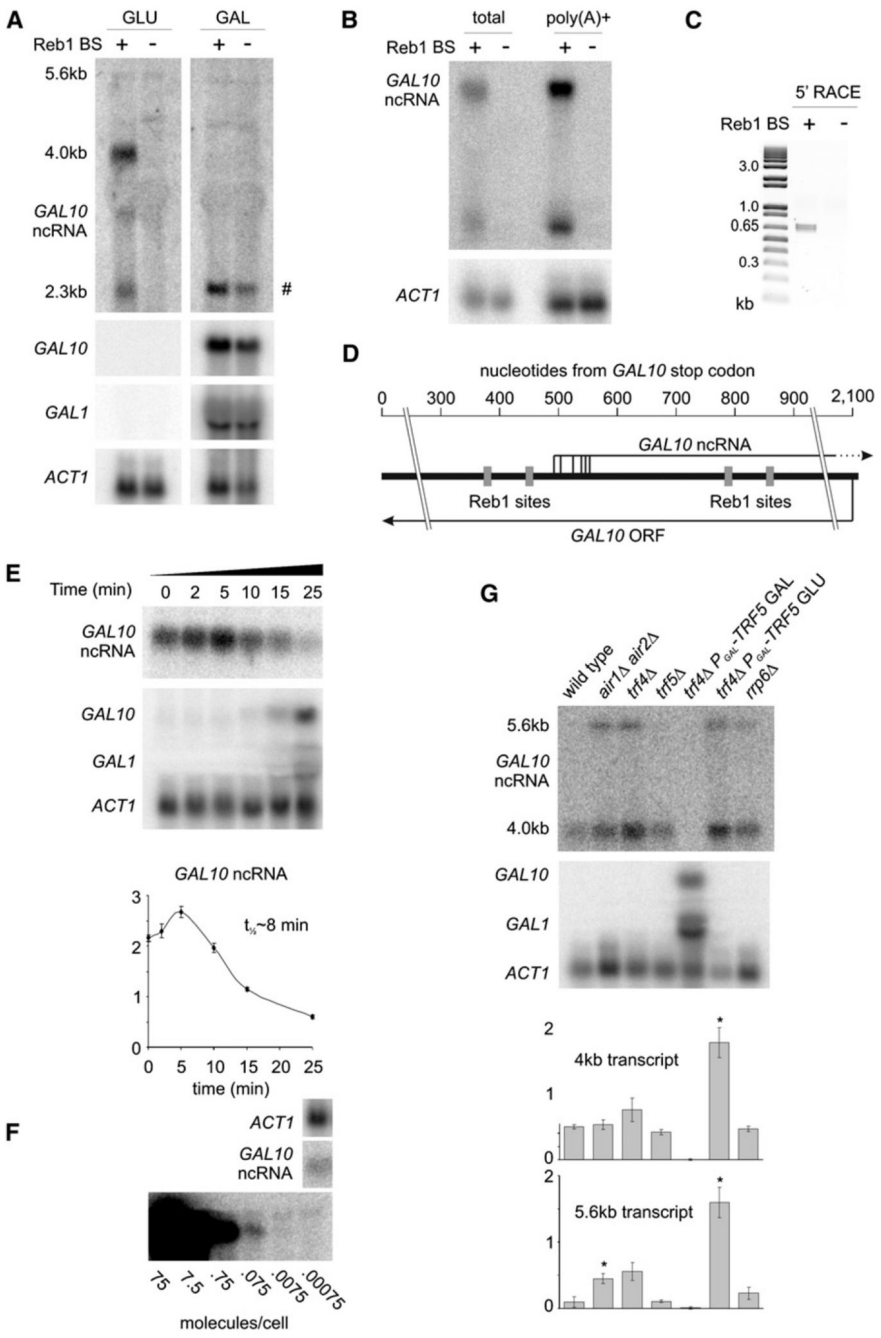

Figure 3. A Cryptic Transcript Is Produced from the 3′ End of *GAL10*

(A) Northern analysis of RNA from wild-type and Reb1 BSΔ mutant cells grown in rich media containing 2% glucose or 2% galactose. Probes are *GAL10* sense, *GAL10* antisense, *GAL1, ACT1.* Bands marked # in galactose samples are *GAL10* mRNA, detected since small amounts of antisense RNA probe are produced by template strand switching ("turnaround transcription") at the end of the DNA substrate during in vitro transcription. (B) Total and oligo(dT) affinity selected RNA from wild-type and Reb1 BSΔ mutant cells hybridized with *GAL10* sense and *ACT1* probes.

(C) Cap-dependent 5′ RACE analysis of total RNA performed using a GeneRacer kit with primer GAL10F2. Products were cloned and sequenced to determine transcriptional start site.

(D) Schematic of *GAL10* ncRNA 5′ ends as determined by 5′ RACE.

(E) Quantification of transcript half-life after addition of 2% galactose to cells growing exponentially in raffinose medium. RNA was probed for *GAL10* antisense, *GAL10*, *GAL1*, and *ACT1*. Quantification represents data from three cultures; y axis is in arbitrary units; error bars indicate ±1 standard error.

(F) *GAL10* antisense signal from 20 **m**g FT4 wild-type RNA compared to signal from in vitro transcribed truncated *GAL10* antisense RNA in 20 **m**g of wild-type RNA. Panels showing *GAL10* antisense and the in vitro transcribed RNA derive from the same exposure of the same blot, and no differential processing has been applied.

(G) Northern analysis of *GAL10* antisense in TRAMP mutants. Cells were grown to mid-log phase at 25° in rich media containing 2% glucose, except the *trf4*Δ *GAL-trf5* strain,which was grown on 2% galactose prior to a 24 hr shift to 2% glucose. RNA analysis as in (E). *p < 0.05 for Student's t test of wild-type versus mutant.

Europe PMC Funders Author Manuscripts

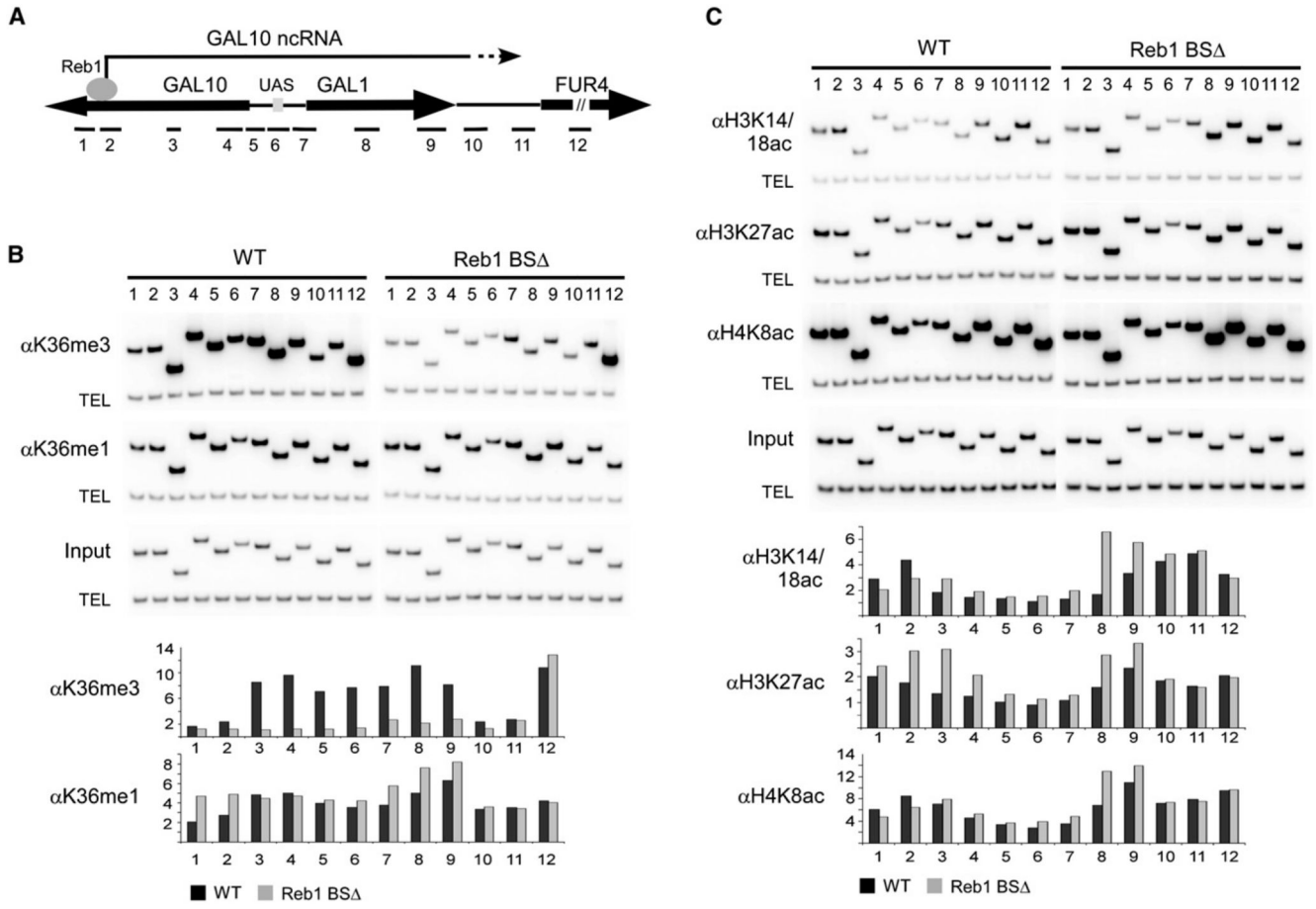

Figure 4. Histone Modifications Induced by the *GAL10* ncRNA

(A) Schematic of the *GAL* locus showing the location of primer sets used for ChIP analysis.

(B) ChIP analysis of H3 K36 methylation in the presence and absence of the *GAL10* ncRNA (Reb1 BS+/−). Cells were grown to log phase in rich media containing 2% raffinose, and chromatin was precipitated with antibodies against H3 K36me3 and H3 K36me1. PCR was performed with primer sets shown on the schematic diagram for the *GAL* locus and a telomeric primer set (TEL) as a loading control.

(C) ChIP analysis of histone acetylation in the presence and absence of the *GAL10* ncRNA (Reb1 BS+/−). Cells were grown to log phase in rich media containing 2% raffinose, and chromatin was precipitated with antibodies against acetylated H3 K14/18, H3 K27, and H4 K8. PCR was performed with primer sets shown on schematic diagram for the *GAL* locus and a telomeric primer set (TEL) as a loading control.

Graphs in (B) and (C) show quantification of ChIP data as fold enrichment of signal at the *GAL* locus over telomeric signal normalized to the input. Data shown is the average of two independent experiments.

Europe PMC Funders Author Manuscripts

Europe PMC Funders Author Manuscripts

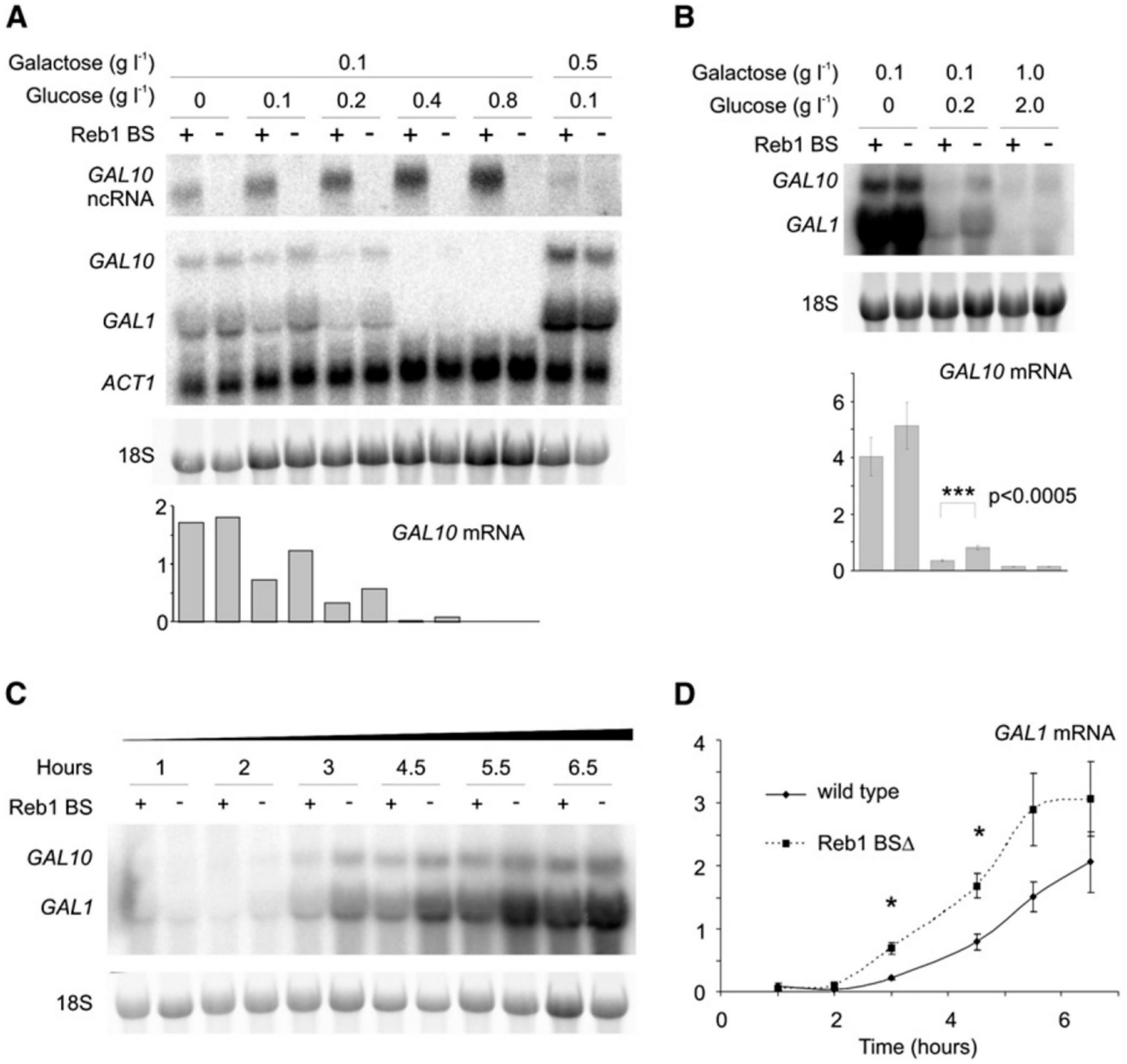

Figure 5. The Effect of *GAL10* ncRNA Expression on Glucose Repression

(A) *GAL* induction in response to low-galactose/glucose mixtures. Cells were grown to OD ~0.4 in 2% raffinose, and then glucose and galactose were added to the indicated concentration. Cells were harvested after 3 hr, and RNA was probed for *GAL1, GAL10*, and *ACT1*, and for the *GAL10* ncRNA. The 18S rRNA signal is from ethidium staining. Quantification of *GAL10* mRNA levels was determined relative to *ACT1* signal. The increasing level of 18S and *ACT1* with increasing glucose concentrations is due to the elevated growth rate.

(B) Quantification of *GAL* induction. Cells were grown to OD ~0.4 in 2% raffinose, and then glucose and galactose were added to the indicated concentration. Cells were harvested

after 2 hr, and RNA was probed for *GAL1* and *GAL10*. Data were normalized to 18S ribosomal RNA levels determined by ethidium staining. Quantification represents data from six cultures; y axis is in arbitrary units; error bars indicate ±1 standard error.

(C) Cells were grown overnight to OD ~0.2 in rich 2% raffinose media; no dilution or manipulation of the cultures was performed prior to the experiment. Cultures were induced with 0.1 g l^{-1} galactose/0.2 g l^{-1} glucose, and samples were taken at the indicated time points. RNA analysis as in (B).

(D) Quantification of time course data from (C). Data are from three cultures; y axis is in arbitrary units; error bars indicate ±1 standard error. * $p < 0.05$ for Student's t test of wild-type versus mutant.

Europe PMC Funders Author Manuscripts

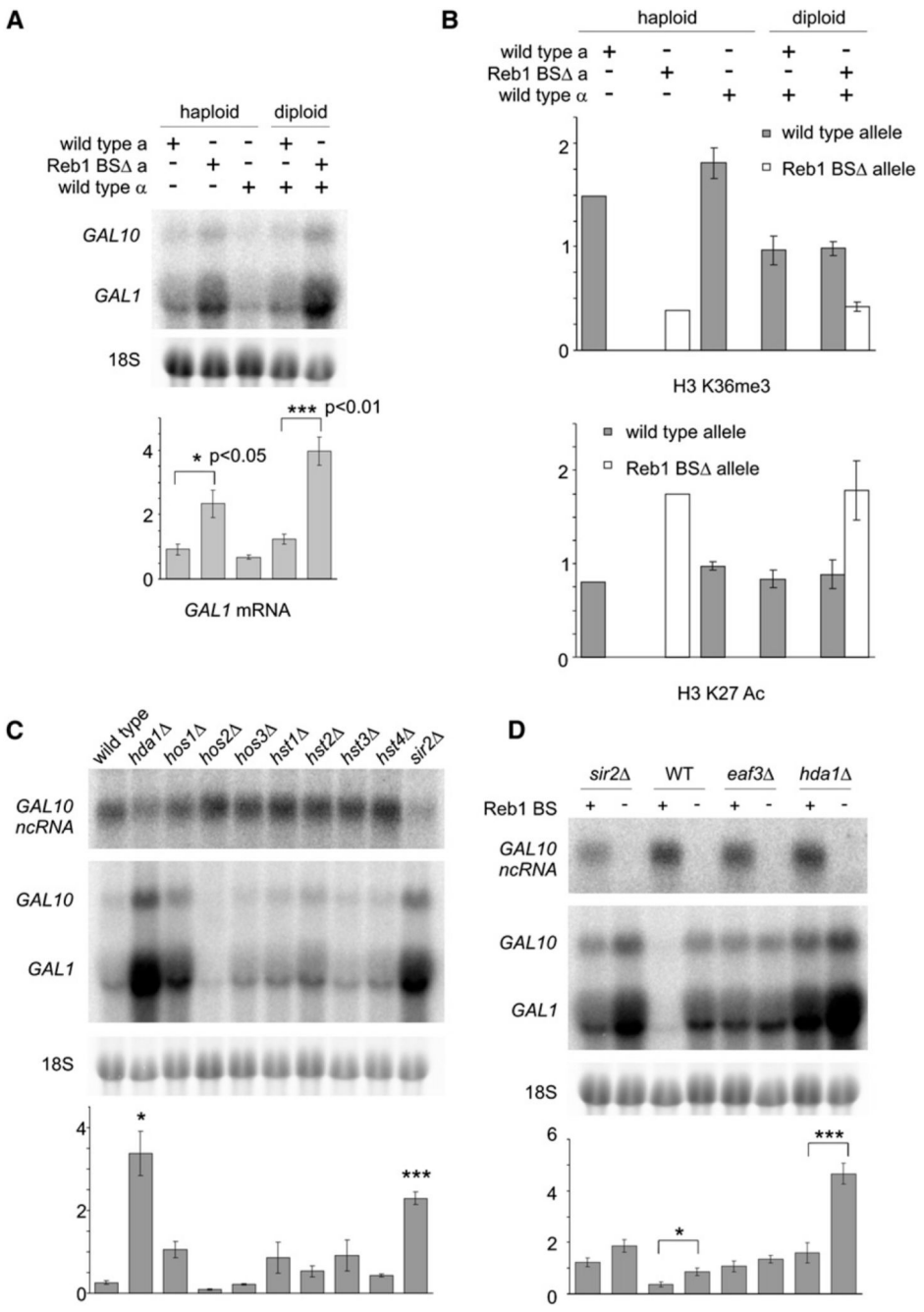

Figure 6. Mechanistic Analysis of *GAL10* ncRNA's Role in Glucose Repression

(A) *GAL* induction in haploid and diploid strains. Analysis of three haploid parental strains (FT4, Reb1 BSΔ-silent, and BY4742) and two diploid strains (FT4 x BY4742 and Reb1 BSΔ-silent x BY4742), grown overnight to OD ~0.2 in rich 2% raffinose media and induced with 0.1 g l^{-1} galactose/0.2 g l^{-1} glucose. Cells were harvested after 3 hr, and RNA was analyzed and quantified as in Figure 5B. Quantification represents data from four cultures of each strain.

Europe PMC Funders Author Manuscripts

(B) Allele-specific ChIP analysis of H3 K36 trimethylation and H3 K27 acetylation at the 5′ end of *GAL10* ncRNA in cells grown in 2% raffinose. One replicate of FT4 and Reb1 BSΔ-silent and three replicates each for BY4742 and the two diploid strains were performed. PCR product normalized to loading control (Tel) and input DNA are shown for each allele in each strain; error bars indicate ±1 standard deviation.

(C) Analysis of GAL gene induction in histone deactylase mutants. Cell growth, induction, and analysis as in (A). *GAL10* ncRNA is visualized with probe to *GAL1*/*GAL10*. Quantification represents data from three cultures of each strain; error bars indicate ±1 standard deviation.

(D) Analysis of GAL gene induction in HDAC mutants combined with Reb1 BSΔ. Cell growth, induction, and analysis as in (C). Quantification represents data from seven cultures in two experiments (WT, *sir2*Δ, and *eaf3*Δ strains) and from three cultures in one experiment (*hda1*Δ strains); error bars indicate ±1 standard deviation.

Europe PMC Funders Author Manuscripts

Europe PMC Funders Author Manuscripts

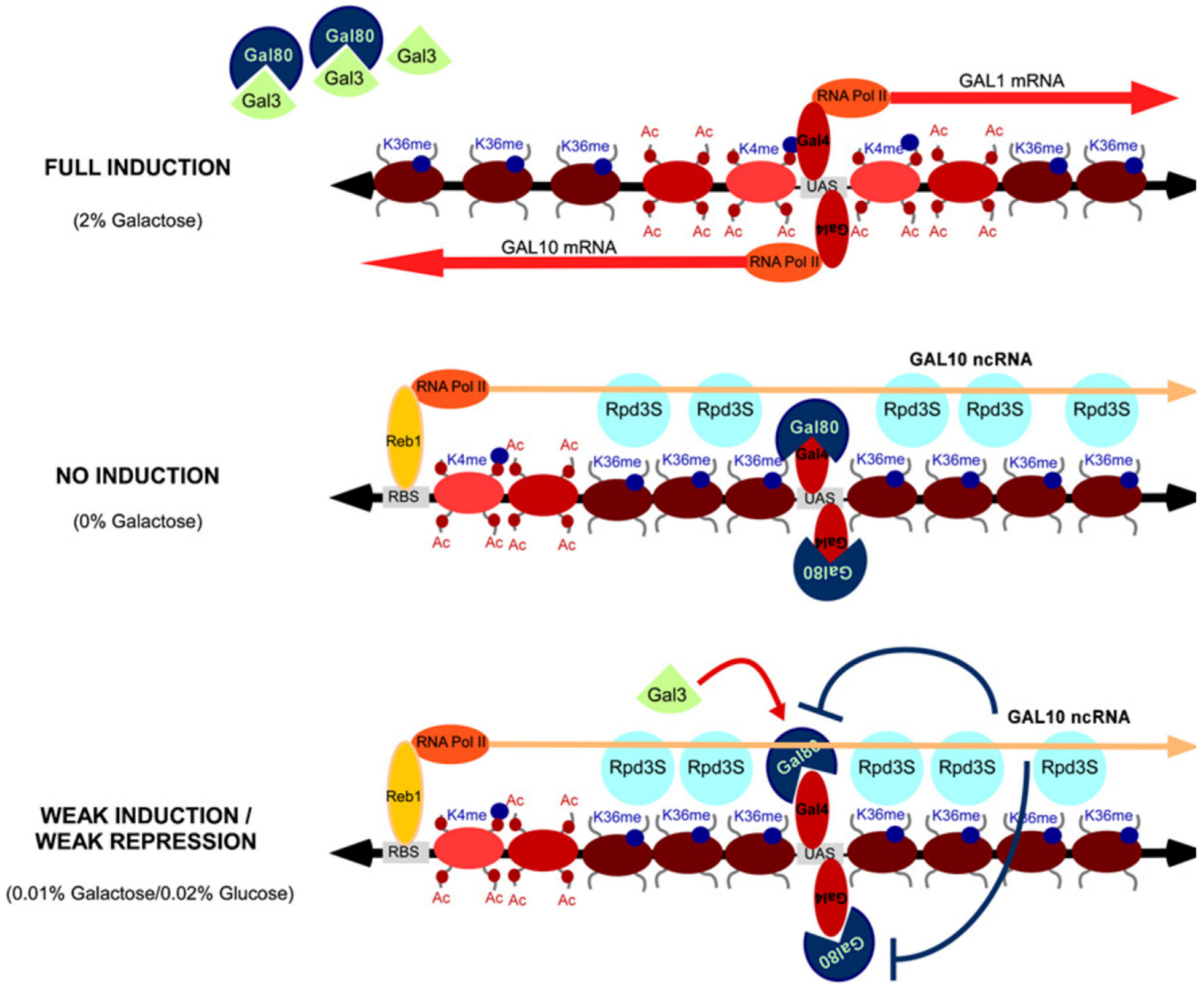

Figure 7. Model for *GAL10* ncRNA-Induced Histone Modifications over the GAL Cluster

Full induction: *GAL1–10* are transcribed. Reb1 binding to the *GAL10 3* is absent, and no ncRNA is produced. No induction: *GAL1–10* are not transcribed. Reb1 binds within the *GAL10* coding region and induces *GAL10* ncRNA transcription. This results in high levels of K36me3 and increased histone deacetylation over the *GAL1–10* cluster. Weak induction/ weak repression: *GAL10* ncRNA-induced chromatin modifications repress *GAL1–10* transcription in condition of concomitant weak induction and repression.